Polish J. Chem., **70**, 1018–1029 (1996)

2′-Deoxycytidine Hemidihydrogenphosphate: Comparison of Crystal Structure Refinements Based on Diffractometer and Image Plate Data

by Z. Dauter[1] and M. Jaskólski[2]*

[1]*EMBL, c/o DESY, Notkestrasse 85, 22603 Hamburg, Germany*
[2]*Department of Crystallography, A. Mickiewicz University and Center for Biocrystallographic Research, Polish Academy of Sciences Poznań, Poland*

(Received January 5th, 1996; revised manuscript March 28th, 1996)

The crystal structure of 2′-deoxycytidine hemidihydrogenphosphate has been refined using diffractometer Cu$K\alpha$ data and imaging plate (IP) Mo$K\alpha$ data collected for the same single crystal. The IP Mo data were collected 55 times more efficiently, extend to higher resolution, and resulted in a more precise (1.6 times) structural model which revealed fine features (related to H-atom location) impossible to derive from the Cu data. Even though a δF (data set 1 *vs.* data set 2) normal probability plot indicates that there are systematic differences between the two data sets, the individual δR (F_0 *vs.* F_c) plots reveal that this systematic error has been absorbed by the structural model(s). When structural models derived from the two data sets were compared, the δp normal probability plots showed a systematic shift in the displacement parameters but no drastic systematic differences in the positional parameters. A comparison of two structural models based on the same (IP Mo) data revealed agreement between the displacement parameters and systematic differences in the positional parameters. The refinements demonstrate that care must be exercised when interpretating fine (and often problematic) structural features (like minor sites in disordered systems) because they may be influenced by the quality of the experimental data.

Key words: crystal structure, disorder, hydrogen bond

Two-dimensional X-ray detectors capable of simultaneously measuring many reflection intensities were originally designed for macromolecular crystallography. The past few decades have witnessed the introduction and development of position-sensitive ionization area detectors, TV-camera detectors, imaging plates, and, more recently, of CCD detectors. The early area detector designs provided only medium-quality intensity data. However, continuous improvement of crystallization techniques, which can today produce very high quality macromolecular crystals, stimulated a rapid progress in detector technology and developments in the software for processing their output. Using both scintillation-type automatic diffractometers and image plate detectors for small-molecule and macromolecular diffraction experiments, we came to the conclusion that the imaging plate technique has now reached the quality standard typically associated with single crystal diffractometers. To compare these two techniques, we have refined a small-molecule structure using intensity data collected on a Syntex $P2_1$ single crystal diffractometer and using a Mar 180 mm image plate detector. The structure selected for these comparisons was

* Corresponding author.

2'-deoxycytidine hemidihydrogenphosphate [1]. All experiments were carried out using one single crystal which originally provided high quality Cu diffraction data on a single crystal diffractometer.

In the analysis below we demonstrate that the quality of the data collected using the image plate detector matches or exceeds that characterizing diffractometer data. The two structural models show a general agreement typical of independent structure determinations and differ only in structural details which are problematic in themselves. The structure derived from the image plate data has a markedly better precision (by a factor of 1.6) and reveals subtle details impossible to derive from the diffractometer data.

EXPERIMENTAL

Intensity data and structural models: All diffraction experiments were carried out on a single crystal with dimensions 0.31 × 0.31 × 0.36 mm. The crystal, obtained from methanol/water mixture (3:1), had hexagonal bipyramidal habit and well developed natural faces. The space group is $P6_2$ with a = 25.839(3), c = 12.529(1) Å (unit cell parameters determined from 15 reflections measured on a diffractometer [1]). The unit cell is relatively big [7244(1) Å^3] and contains Z = 12 formula units, *i.e.* 74 independent non-H atoms. The experimental procedures are compared in Table 1.

Table 1. Crystallographic data, experimental details and refinement details for the diffractometer and image plate experiments.

	Diffractometer Syntex $P2_1$	Image plate Mar 180 mm
Crystal data		
Space group	$P6_2$	$P6_2$
a (Å)	25.839(3)	25.93[a]
c (Å)	12.529(1)	12.60[a]
Axial ratio (a/c)	2.0623(3)	2.058
Temp. (K)	291	291
Crystal size (mm)	0.31 × 0.31 × 0.36	0.31 × 0.31 × 0.36
Linear absorption coeff. (mm^{-1})	μ_{Cu} = 1.66	μ_{Co} = 0.18
Intensity measurements		
Data coll. technique	background-peak-background	rotation method
Wavelength	1.54178 (Cu$K\alpha$)	0.71073 (Mo$K\alpha$)
Resolution, d_{min} (Å)	0.92	0.82
Reflections measured	3735	19168
Unique reflections	3450	4792
Redundance	1.08	4.00
R_{int}	0.026	0.025
Structure refinement		
Parameters refined	683[b]	739[c]
Geometrical restraints	7	4
Accepted reflections	3236	4792
Acceptance criterion	$F \geq 3.92\,\sigma(F)$	$F \geq 0.0\,\sigma(F)$
Function minimized	$\Sigma w(F_o - F_c)^2$	$\Sigma w(F_o - F_c)^2$
Weighting scheme	$w^{-1} = \sigma^2(F) + 0.0005F^2$	$w^{-1} = \sigma^2(F)$

Table 1 (continuation)

Extinction correction	3 reflections excluded	$F' = F(1+ xF^2/\sin 2\theta)^{-1/4}$ $x = 36(4)\cdot 10^{-7}$
R	0.0420	0.0441
wR	0.0578	0.0511
S	2.05	1.88
$\overline{\sigma}$(C–C) (Å)	0.0090	0.0055
$\Delta\rho_{min}$ (eÅ^{-3})	–0.22	–0.30
$\Delta\rho_{max}$ (eÅ^{-3})	0.70	0.82

[a]biased due to approximate calibration of crystal-to-image distance.
[b]model I_{Cu}.
[c]model II_{Mo}.

The structure was originally solved and refined using diffractometer data by Jaskólski *et al.* [1]. It has a peculiar architecture consisting of tightly hydrogen-bonded dihydrogenphosphate anions located on all two-fold axes in the unit cell and of perpendicular cationic layers attached to the phosphate "joints" every c/3. Each cationic layer is composed of two (*AB* and *CD*) cationic dC$^{\oplus}$·dC dimers (dC = 2′-deoxycytidine) (Fig. 1). In all structure refinements (carried out using SHELX76 [2] and SHELXTL [3] on an IBM PC computer) the function minimized was $\Sigma w(F_0 - F_c)^2$. The normal probability plots for comparisons of structure factors and model parameters were generated using a program written by MJ.

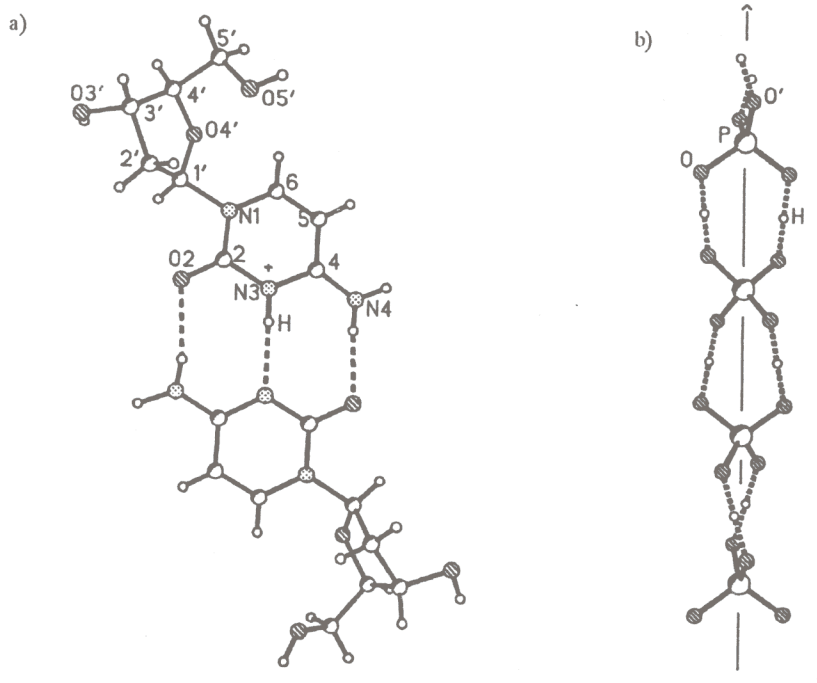

Figure 1. The structural motifs composing the crystal structure of 2′-deoxycytidine hemidihydrogenphosphate [1]. (a) Cationic hydrogen-bonded dC$^{\oplus}$·dC base pairs; there are two such dimers, *AB* and *CD*, in the asymmetric unit. (b) Columns of hydrogen-bonded $H_2PO_4^-$ anions; two different two-fold-symmetric columns are present in the asymmetric unit: one is formed by the P(1)-phosphate located on the 6_2 screw, while the other is composed of repeating P(2)-, P(3)-, and P(4)-phosphates.

Diffractometer data: The data were collected on a Syntex $P2_1$ diffractometer using sealed-tube Cu radiation and graphite monochromator [$\mu(CuK\alpha) = 16.6$ cm^{-1}] at $T = 291$ K (Table 1). The intensities were determined in the background-peak-background mode using a variable rate (between 2.0 and 29.3°/min) θ–2θ scan. The 2θ scan range was 2° plus $\alpha_1 - \alpha_2$ split. The stationary background measurements for each reflection were made at the low- (t/4 sec) and high-angle (t/4 sec) limit of the scan range which was integrated in 96 steps during t seconds. A total of 3735 reflections were collected for $4 \leq 2\theta \leq 114°$ and $0 \leq h \leq 28$, $0 \leq k \leq 28$, $0 \leq l \leq 13$. The upper 2θ limit approximately corresponds to the maximum angle available on a Syntex $P2_1$ diffractometer operating in the bisecting mode and determines the maximum resolution of Cu data as 0.92 Å. The total duration of the intensity measurements was 75 hours. Averaging of symmetry-related reflections resulted in 3450 unique data with $R_{int} = 0.026$, comparable with the intensity variation of 3% displayed by two frequently measured reference reflections. The refinements were carried out using 3236 observed reflections with $I \geq 1.96\sigma(I)$ but excluded three strong reflections (220, 240, 420) suspected of high extinction. The weighting scheme was $w^{-1} = \sigma^2(F) + 0.0005F^2$. Persistent difference-Fourier peaks within the side chain regions of sugars *A* and *C* suggested disorder of the corresponding O(5') atoms. The model was therefore adjusted to accommodate split O(5'*A*) and O(5'*C*) atoms. The partial occupancies were fixed at proportions which gave similar displacement parameters of the split components [0.7/0.3 at O(5'*A*), 0.9/0.1 at O(5'*C*)]. In the final model all non-H atoms were treated anisotropically, except for the low-occupancy O(5'*C*) atom which was refined isotropically. To improve the geometry of the disordered C(5')–O(5') groups, seven weak geometrical restraints were included in the final refinement. The C–H hydrogen atoms were included at calculated positions. All N–H hydrogen atoms were located in a difference-Fourier map. All hydroxyl H atoms [except those in the disordered O(5'*C*) group and at the low-occupancy O(5'*A*) component] were located in ΔF maps. The 2'-deoxycytidine H atoms were given (fixed) B_{iso} values one unit greater than B_{eq} of their carriers on which they were riding during the refinement. The H atoms of the $H_2PO_4^-$ groups posed a special problem. Because of the short lengths of the interphosphate O···O hydrogen bonds it might be expected that those H atoms could be located close to, or disordered on both sides of, the midpoints of the O···O distances. All attempts to refine ΔF peaks as possible phosphate H atoms failed. Finally, the phosphate H atoms were fixed with $B_{iso} = 0.1$ Å^2 at the centers of their corresponding O···H···O hydrogen bonds. The refinement of this model (I_{Cu}) converged with $R = 0.0420$, $wR = 0.0578$ and $S = 2.05$ for 3236 reflections. The final ΔF map had electron density between –0.22 and 0.70 e.Å^{-3} and the average σ(C–C) was 0.0090 Å [1] (Table 1).

Image plate data: The data were collected using a Mar 180 mm image plate (IP) detector, sealed-tube Mo source and graphite monochromator [m(Mo$K\alpha$) = 1.8 cm^{-1}] at $T = 291$ K (Table 1). The rotation method [4] was employed, as is routine in macromolecular crystallography. To overcome the limitation of the dynamic range of the image plate, two sets of images were collected with different exposures. The first set consisted of 45 images with 2° oscillation per image at 70 mm crystal-to-detector distance and 5 min exposures. Reflections were accepted in the resolution range 5.0–0.82 Å. The second set was collected with 3° oscillation (30 images) at 170 mm distance and 1 min exposure within the resolution range 10.0–1.5 Å. The crystal was mounted with its b*-axis almost parallel to the spindle axis of the camera and, therefore, a 90° quadrant of the reciprocal lattice between a*b*- and b*c*-planes was covered in both data sets, leading to three copies of the asymmetric part recorded on the detector.

The images were interpreted and intensities integrated using program DENZO [5] on a VAX 3100 workstation yielding a 97.6% complete data set of 4792 unique reflections (4911 expected). The data statistics in resolution shells are presented in Fig. 2. The IP experiments were completed within 7 hours and resulted in a data set with average redundance of 4.0. In view of this and the difference in resolution, the image plate scanner collected data *ca.* 55 times more efficiently than the diffractometer. Overall $R_{int} = 0.025$ and reaches 0.110 in the highest resolution range. The cell constants derived from image processing are $a = 25.93$, $c = 12.60$ Å. Their inaccuracy results from lack of precise calibration of the crystal-to-image distance. The *a*/*c* axial ratio (2.058) is in reasonable agreement with the value of 2.0623(3) derived from diffractometer measurements. For the final analysis, the more precise unit cell parameters from diffractometer measurements were used.

The initial refinement using IP data was carried out for a model constructed exactly as I_{Cu}. The only differences in the refinement protocol were in the treatment of the diffraction data: (i) no sigma cut-off was used, (ii) the weighting scheme was $w^{-1} = \sigma^2(F)$, (iii) instead of excluding extinction-affected reflections, an empirical isotropic extinction correction x was applied to the calculated structure factors [$F' = F(1 + xF^2/\sin 2\theta)^{-1/4}$] which refined to $x = 71(9) \times 10^{-7}$. Refinement of this model (designated I_{Mo}) converged at $R = 0.0438$, $wR = 0.0524$, and $S = 1.92$ for 4792 reflections. The final ΔF map had features

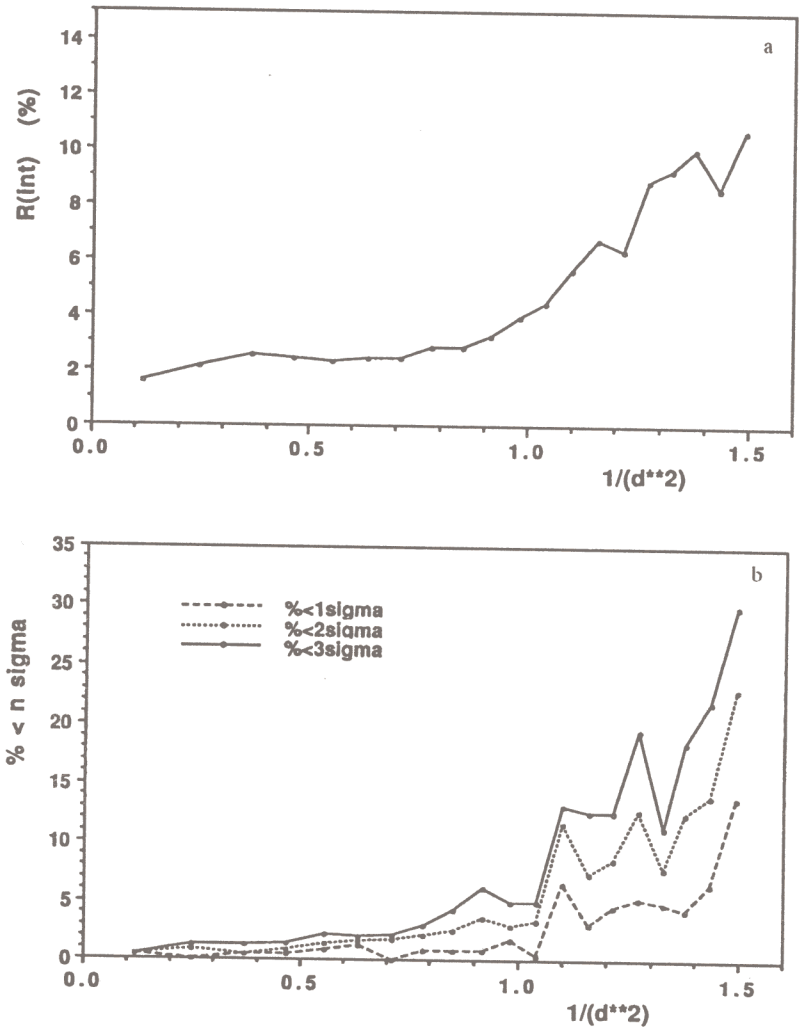

Figure 2. Image plate data statistics. (a) R_{int} *vs.* resolution; (b) percentage of reflections below specified $\sigma(I)$ limit.

between –0.25 and 0.84 e.Å^{-3} and the average σ(C–C) was 0.0056 Å. While the B_{eq} parameters of the split O(5′*A*) atom remained similar [0.133(4) Å^2 (0.7), 0.117(11) Å^2 (0.3)], those of O(5′*C*) did not [0.100(2) Å^2 (0.9), 0.054(6) Å (0.1)]. Therefore, a slightly modified version of that model was generated (I'_{Mo}) in which the occupancies of the split O(5′*C*) atom were fixed at 0.8/0.2. Refinement of I'_{Mo} resulted in a more balanced situation at O(5′*C*) 0.089(2) Å^2 (0.8), 0.106(6) Å^2 (0.2)] and in marginally better convergence parameters [R = 0.0434, wR = 0.0518, S = 1.89, average σ(C–C) = 0.0055 Å]. To assess the validity of the problematic features of models I_{Mo} and I'_{Mo}, another model II_{Mo}, was constructed based on the IP data. To this end, the positional parameters of all N–H hydrogen atoms were allowed to vary, the low-occupancy components of the O(5′) atoms as well as all O–H hydrogen atoms were removed and several cycles of least-squares refinement were calculated in which the diffraction data were treated as above. The subsequent ΔF maps revealed the minor component of the O(5′*A*) atom but gave poor and conflicting evidence of disorder at the O(5′*C*) site. Consequently, the O(5′*A*) atom was split into two anisotropic sites (occupancies 0.65 and 0.35) the displacement parameters of which were characterized

in the final refinement by B_{eq} of 0.122(4) and 0.130(11) Å^2, respectively. The ΔF maps also indicated the positions of all the hydroxyl H atoms of the sugar moieties, except for the minor O(5'*A*) component. All those H atoms [except that in the disordered O(5'*A*) hydroxyl] were subject to refinement with fixed B_{iso} (one unit greater than B_{eq} of their O atoms) with only very loose restraints imposed on O(3'*A*)-H and O(5'*C*)–H. The final geometry of the hydroxyl groups is very good with the O–H distances ranging from 0.89(6) to 1.11(7) Å [average 0.96(3) Å]. The *exo*-amino H atoms also refined with good geometry, the N–H distances ranging from 0.80(7) to 1.22(5) Å [average 0.93(4) Å]. The two H atoms at the protonation sites refined to N(3)–H distances of 0.92(5) Å (in *A*) and 0.89(4) Å (in *C*). The quality of the data allowed to locate the $H_2PO_4^-$ hydrogen atoms, except that in the P(1) phosphate (occupying the 6_2 axis). When included in the refinement (with B_{iso} fixed at 0.1 Å^2), those H atoms were very well behaved, in contrast to the situation in the I_{Cu} model and diffractometer data. Surprisingly, but in agreement with the chemical nature of the hydrogen-bonded phosphate O atoms, the H atoms were pulled out from the central positions in the P–O···O–P bridges and remained stable closer to those O atoms which have longer P–O distances. The results are illustrated in Table 2. Even though the differences between the two P–O bonds in the individual P(2), P(3), P(4) phosphates are not very significant, their correlation with the O–H/H···O differences is a remarkable result of this Mo-data structure refinement. Also, the equalization of the P(1)–O bond lengths may provide an explanation why the attempts to locate and refine the H(1) atom have been unsuccessful. The refinement of the II_{Mo} model converged with R = 0.0441, wR = 0.0511 and S = 1.88 for 4792 reflections. The isotropic extinction parameter refined to $x = 36(4)\times10^{-7}$ and the final ΔF map had features between –0.30 and 0.82 e.Å^{-3}. The highest difference peaks were located within the disordered C(5'*A*)–O(5'*A*) group while in the O(5'*C*) region there was no indication of any significant disorder (highest peak 0.18 e.Å^{-3}). The average σ(C–C) of the II_{Mo} model is 0.0055 Å (Table 1).

Lists of structure factors corresponding to the IP measurements, as well as of atomic coordinates and displacement parameters characterizing the II_{Mo} model, have been deposited in the Faculty of Chemistry, A. Mickiewicz University, Poznań, Poland, and are available on request.

Table 2. Geometry of the H bonds and P–O distances within the phosphate columns in the II_{Mo} model.

P(n)	P(n)–O(n1)	P(n)–O(n2)	H(nm)	O(n2)–H	H···O(m1)'	O(n2)···O(m1)'		P–O–H	O–H···O
	Å	Å		Å	Å	II^a_{Mo} Å	I^b_{Cu} Å	°	°
P(1)	1.535(2)	1.532(2)	H(1)[c]			2.498(3)	2.499(5)		
P(2)	1.517(4)	1.520(3)	H(23)	1.12(7)	1.45(7)	2.547(4)	2.550(6)	110(3)	164(5)
P(3)	1.528(3)	1.534(2)	H(34)	1.03(7)	1.47(7)	2.489(3)	2.488(6)	115(3)	166(3)
P(4)	1.524(3)	1.537(2)	H(42)	0.79(7)	1.75(7)	2.502(4)	2.500(6)	103(4)	158(4)

[a]Results of refinement based on IP Mo data.
[b]Results of refinement based on diffractometer Cu data [1].
[c]Not located.

DISCUSSION

The method of normal probability plot developed by Wilk and Gnanadesikan [6] and introduced to crystallography by Abrahams and Keve [7] is a convenient tool for testing if the differences between individual data points in two (usually large) data sets are random (*i.e.* have normal distribution) or not. We have applied this method to compare the two sets of experimental structure factors (δF plot) and to compare each of them with the corresponding set of calculated structure factors (δR plots). Similarly, δp plots have been used to compare the parameters of the structural models.

Fig. 3 is a δF normal probability plot illustrating the differences $(|F_0^{Cu}| - k|F_0^{Mo}|) / [\sigma^2(F_0^{Cu}) + k^2\sigma^2(F_0^{Mo})]^{1/2}$. The normalizing variances were those used in the least-squares structure refinements. Thus, $\sigma^2(F_0^{Mo})$ corresponds to the experimental variances while $\sigma^2(F_0^{Cu})$ includes the additional term, $0.0005F^2$. In both data sets all reflections were considered (no sigma cut-off). The plot deviates from linearity, particularly in its positive half, and has a large intercept (–0.483). These facts are discouraging, because they demonstrate that one of the data sets, or both, contains systematic errors. It is not obvious what the source of this error is. To some extent, it could be explained by an absorption error, present in the Cu data in spite of the moderate absorption coefficient and fairly regular crystal shape. The general slope of the least-squares line through the data points (1.761) indicates, that the joint standard deviations of the structure factors, $(\sigma_1^2 + \sigma_2^2)^{1/2}$, are systematically too low.

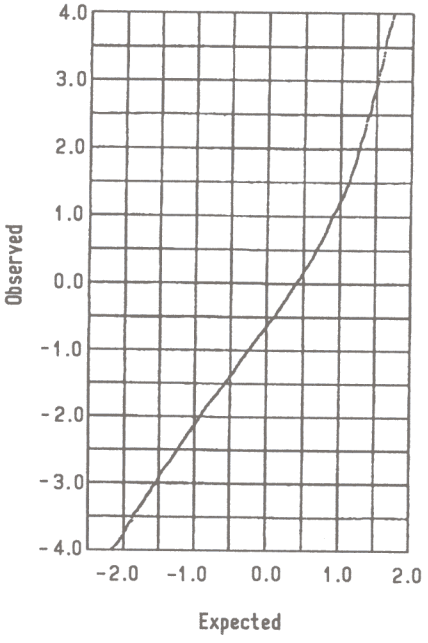

Figure 3. Normal probability plot generated from $\sigma F = (|F_0^{Cu}| - k|F_0^{Mo}|) / [\sigma^2(F_0^{Cu}) + k^2\sigma^2(F_0^{Mo})]^{1/2}$. The two data sets (3452 Cu data, 4792 Mo data) had 3373 common reflections of which 191 had $|\delta F| > 4$ and are not plotted. The least-squares line through the remaining 3182 points (correlation coefficient 0.986) has a slope of 1.761 and an intercept of –0.483.

Interestingly, the two δR plots (Fig. 4) are much more linear (their deviations from linearity being very similar) and deviate much less from the origin. Taken individually, the δR plots might suggest that the data sets are free from significant systematic errors. It is only in the δF plot that this bias becomes visible. Therefore, the systematic error present in one of the data sets (or in both) is clearly absorbed in the refined model(s). The general inclination of the two δR plots is very similar and indicates that in both experiments the standard deviations of the structure factors were underestimated by a factor of 1.6.

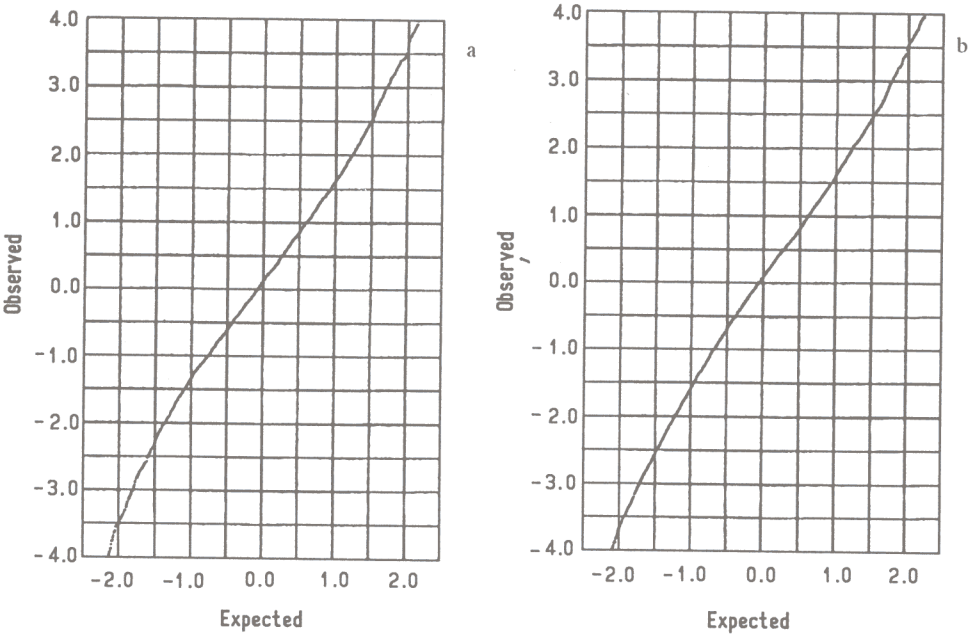

Figure 4. Normal probability plots generated from $\delta R = (|F_0| - |F_c|)/\sigma(F_0)$. In both plots all reflections were included and the variances were those used for weighting in the least-squares refinements. (a) Diffractometer Cu data; 3452 points of which 111 beyond 4 (excluded); the least-squares line through the 3341 points (correlation coefficient 0.997) has a slope of 1.589 and an intercept of 0.123. (b) IP Mo data; 4792 points of which 150 beyond 4 (excluded); the least-squares line through the 4642 points (correlation coefficient 0.998) has a slope of 1.656 and an intercept of 0.037.

Fig. 5 illustrates a comparison of the two data sets in real space by means of δp plots for the non-H atoms of models I_{Cu} and II_{Mo}. The plot which includes both the positional and anisotropic displacement parameters (Fig. 5a) is quite linear but deviates significantly from the origin, indicating that the differences between the parameters of the two models have a systematic component. This systematic bias revealed by a large intercept is even more pronounced in the plot comparing the displacement parameters, although the linearity here is also satisfactory (Fig. 5b). This systematic bias corresponding to a parallel shift of the $\delta U_{ij} = (U_{ij}^{II_{Cu}} - U_{ij}^{II_{Mo}})$ plot may indicate that the displacement parameters of the I_{Cu} model are systematically higher than those in II_{Mo}. This in turn might be explained by an absorption error of the Cu data. Even though the linearity of the plot corresponding to only positional parameters is somewhat poorer (Fig. 5c), its general shape and small intercept indicate that there are no serious systematic differences in the geometry of models I_{Cu} and II_{Mo}. The slopes of all three plots in Fig. 5 are close to unity suggesting that the standard deviations in the parameters estimated in the least-squares calculations are quite reliable.

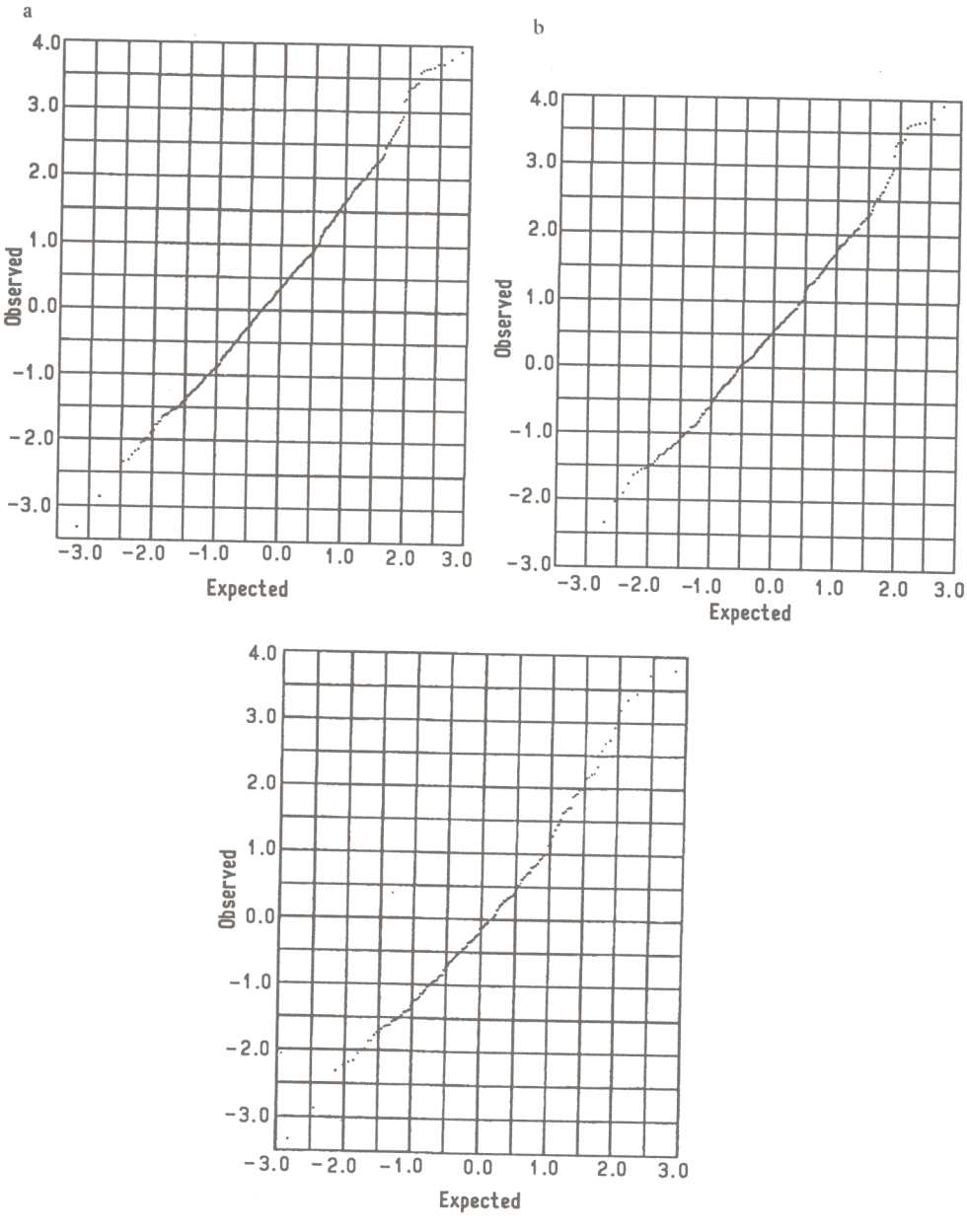

Figure 5. δp Plots of normalized differences between structural parameters of non-H atoms of models I_{Cu} and II_{Mo}. The plots exclude the disordered O(5′*A*) and O(5′*C*) atoms. (a) and $p = x, y, z$ and U_{ij}; 649 parameters considered; the least-squares line through the 648 points not exceeding 4 (correlation coefficient 0.997) has a slope of 1.229 and an intercept of 0.389. (b) $p = U_{ij}$; 436 points corresponding to the components of the anisotropic displacement parameters considered; the least-squares line through the 435 points not exceeding 4 (correlation coefficient 0.996) has a slope of 1.148 and an intercept of 0.597. (c) $p = x, y, z$; the least-squares line through the 213 points corresponding to the positional parameters (correlation coefficient 0.991) has a slope of 1.272 and an intercept of –0.039.

While the above two models (I_{Cu} and II_{Mo}) based on different data sets compared (at least in the geometrical part) reasonably well and showed understandable δp deviations, the comparison of the two models derived from the same (IP Mo) data set (I'_{Mo}, II_{Mo}) presented in Fig. 6 leads to striking and unexpected results. The positional δp plot (Fig. 6c) indicates significant non-random differences between the two models. On the other hand, the δU_{ij} plot (Fig. 6b) is fairly linear and not far from the origin and even indicates that the standard deviations of the displacement parameters are overestimated by a factor of 2. The results of the comparison of models I'_{Mo} and II_{Mo} are even more surprising if one recalls that model I'_{Mo} was refined using a strategy nearly identical to that used with I_{Cu} which, in the previous comparison with II_{Mo}, produced quite different results. To some extent, the disparity between the plots in Figs. 5 and 6 can be explained by the fact that the standard deviations (used to normalize the $p_1 - p_2$ differences) of the parameters of model I_{Cu} are by a factor of 1.6 higher and, therefore, may have obscured the differences which showed up only with sufficiently precise data.

CONCLUSIONS

Refinements of the same small molecule crystal structure using data measured by different techniques indicate that the quality of diffraction data collected on an image plate is at least as good as in the case of a standard diffractometer. With suitable X-ray radiation (Mo$K\alpha$) even a small image plate (180 mm) can produce highly resolved data, exceeding in resolution standards typical in diffractometry. There are hardly any disadvantages of the imaging plate technique. Some inconveniences are related to the limits (even though very broad) in the dynamical range which, with strongly diffracting small-molecule crystals, require two sets of images with different exposure times. The requirement for vast disk space and fast computer is no longer a limitation. The biggest advantage of the image plate lies in its capability to collect data very rapidly (tens of times faster than on a diffractometer) without compromising quality. In the present test, the structural model derived from Mo$K\alpha$ image plate data is superior to that obtained with Cu$K\alpha$ diffractometer data in terms of statistical parameters (standard deviations) and structural features (location of hydrogen atoms).

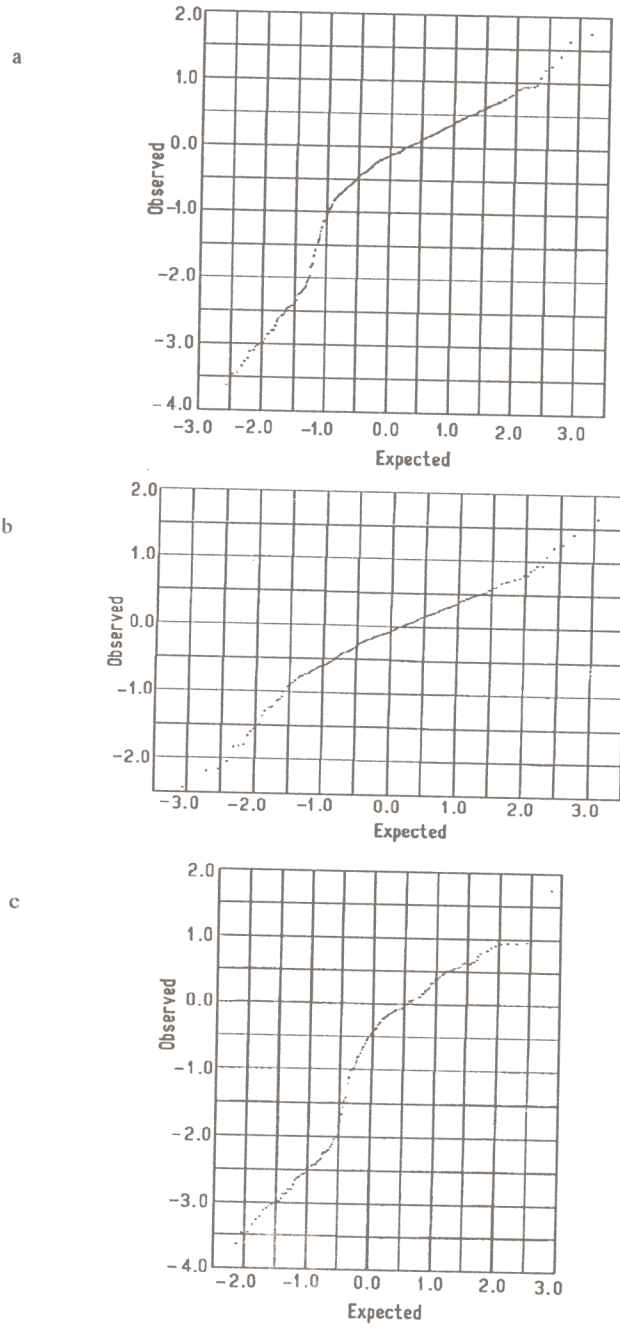

Figure 6. δp Plots of normalized differences between structural parameters of non-H atoms of models I_{Mo} and II_{Mo}. The plots exclude the disordered O(5′*A*) and O(5′*C*) atoms. (a) $p = x, y, z$ and U_{ij}; 649 parameters considered; the least-squares line through the 646 points not exceeding 4 (correlation coefficient 0.927) has a slope of 0.863 and an intercept of –0.369. (b) $p = U_{ij}$; the least-squares line through the 436 points corresponding to the components of the anisotropic displacement parameters (correlation coefficient 0.980) has a slope of 0.535 and an intercept of –0.116. (c) $p = x, y, z$; 213 points corresponding to the positional parameters considered; the least-squares line through the 210 points not exceeding 4 (correlation coefficient 0.959) has a slope of 1.260 and an intercept of –0.903.

Acknowledgement

Research sponsored in part by the Polish State Committee for Scientific Research, grant 2 0661 91 01.

REFERENCES

1. Jaskólski M., Gdaniec M., Gilski M., Alejska M. and Bratek-Wiewiórowska M.D., *J. Biomol. Struct. Dyn.*, **11**, 1 (1994).
2. Sheldrick G.M., SHELX76 Program for crystal structure determination . Univ. of Cambridge, England (1976).
3. Sheldrick G.M., SHELXTL-Plus . Siemens Analytical X-ray Instruments, Inc., Madison, Wisconsin, USA (1989).
4. Arndt U.W. and Wonacott A.J., *The Rotation Method in Crystallography*, North Holland, Amsterdam, 1977.
5. Otwinowski Z., *An Oscillation Data Processing Suite for Macromolecular Crystallograph*, Yale Univ., New Haven, Connecticut, USA (1992).
6. Wilk M.B. and Gnanadesikan R., *Biometrika*, **55**, 1 (1968).
7. Abrahams S.C. and Keve E.T., *Acta Cryst.*, **A27**, 157 (1971).